

Precise Measurement of Matter-Antimatter Asymmetry with Entangled Hyperon Antihyperon Pairs

BESIII Collaboration*

A search for CP violation with an entangled system of $\Xi^- - \bar{\Xi}^+$ pairs is performed, using $(10,087 \pm 44) \times 10^6$ J/ψ events collected with the BESIII experiment. A nine-dimensional helicity amplitude is used to fit $e^+e^- \rightarrow J/\psi \rightarrow \Xi^- \bar{\Xi}^+$ and its subsequent decays. The Ξ^- and $\bar{\Xi}^+$ decay parameters are determined with higher precision compared to the best results reported so far. Furthermore, the strong phase difference, $(\delta_P - \delta_S) = (0.3 \pm 1.2 \pm 0.2) \times 10^{-2}$ rad, and the weak phase difference, $(\xi_P - \xi_S) = (-0.2 \pm 1.2 \pm 0.1) \times 10^{-2}$ rad, are directly determined. These are the most precise measurements to date. The CP asymmetry observables $A_{CP}^{\Xi} = (-7.8 \pm 4.8 \pm 0.8) \times 10^{-3}$ and $\Delta\phi_{CP}^{\Xi} = (0.6 \pm 5.1 \pm 0.2) \times 10^{-3}$ rad are determined, which are consistent with CP conservation. In addition, independent measurements of the Λ decay parameter and CP asymmetry $A_{CP}^{\Lambda} = (-2.9 \pm 4.3 \pm 0.7) \times 10^{-3}$ are also obtained, which are in agreement with the previous measurements, but with much improved precision.

One of the main unresolved puzzles in fundamental physics is to explain how the vast abundance of matter over antimatter in the universe was generated. The most viable explanation is a dynamic mechanism, Sakharov's theory of *baryogenesis* [1]. For such a mechanism to leave a lasting imprint, it must meet a few essential criteria, one of which requires physics processes that violate the combined charge conjugation and parity (CP) symmetry. So far, CP violation has only been discovered in weak flavor-changing quark transitions. Within the Standard Model (SM), it is accounted for through a single irreducible complex phase in the Cabibbo–Kobayashi–Maskawa matrix [2, 3]. However, this mechanism is insufficient to explain the observed matter-antimatter asymmetry of our universe [4, 5]. Experimentally, CP violation has been well established in strange, beauty and charm meson decays [6–9]. Only recently, the LHCb collaboration observed CP violation in a beauty baryon decay, $\Lambda_b^0 \rightarrow pK^-\pi^+\pi^-$ [10]. Since baryons have an additional spin degree of freedom, precise CP measurements test the SM in a complementary way. For non-leptonic two-body weak decays of hyperons, direct CP violation can be compared to that of kaon non-leptonic weak decays [11, 12]. To observe CP violation, there should be two or more weak amplitudes which can interfere with each other. For kaons, the interference effects, that give rise to CP violation, come from the two-pion isospin states $I_{\pi\pi} = 0, 2$. For $\Delta S = 1$ transition in $\Xi^- \rightarrow \Lambda\pi^-$, the two interfering amplitudes come from the parity-odd (S -wave) and parity-even (P -wave) decay amplitudes. For the $L = S, P$ amplitudes, the strong and weak phase components are denoted as δ_L and ξ_L , respectively. The full amplitude is given by $L = \sum_j L_j \exp(i\delta_j^L + i\xi_j^L)$, where j runs over all possible combinations of $[2I, 2\Delta I]$. The coefficient L_j is real, and I and ΔI represent the isospin of the final state and the change of isospin from the initial to final state, respectively [12, 13]. While the strong phases δ_L do not change

sign for the charge-conjugated states, the weak phases ξ_L do.

For a non-leptonic two-body weak decay, the angular distributions of the final-state particles allow for the extraction of three decay parameters α , β and γ , which are described by the S - and P -wave amplitudes [14]. In addition the parameters β and γ can also be described via α and the independent phase angle ϕ , $\beta = \sqrt{1 - \alpha^2} \sin \phi$ and $\gamma = \sqrt{1 - \alpha^2} \cos \phi$. The decay parameters are related to the polarization of the decaying system, as shown in Fig. 1. In the helicity reference system for the decay

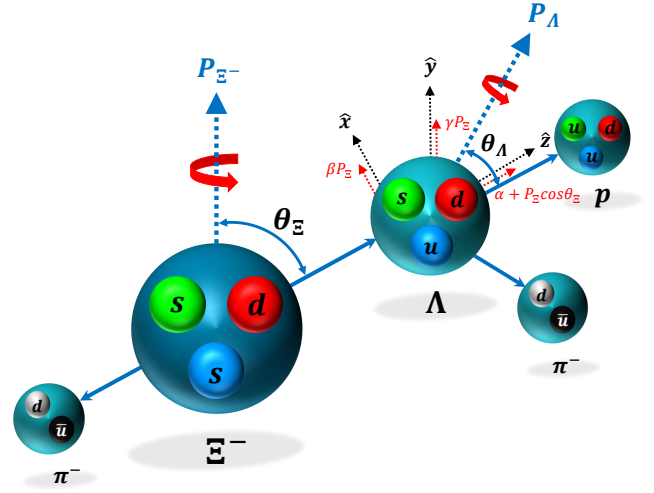


FIG. 1. Illustration of the polarization vectors of Λ and Ξ^- hyperons in relation to the decay parameters α , β , and γ for the $\Xi^- \rightarrow \Lambda\pi^-$ with $\Lambda \rightarrow p\pi^-$ process, in the Ξ^- rest frame.

$\Xi^- \rightarrow \Lambda\pi^-$, the \hat{z} axis is defined by the momentum direction of the final state baryon (Λ) momentum in the Ξ^- rest frame. The \hat{y} axis is defined as the cross product of the \hat{z} axis and the initial polarization $\mathbf{P}_{\Xi} \times \hat{z}$. When decaying, the initial Ξ^- polarization, \mathbf{P}_{Ξ} , is transferred to the final state baryon, both longitudinally and transversely. The longitudinal component depends on both the initial polarization and the value of α_{Ξ} , while ϕ_{Ξ} is

* Full author list given at the end of the Letter.

directly proportional to \mathbf{P}_Ξ . The parameters α_Ξ and ϕ_Ξ are CP -odd and can be used to test the CP symmetry. The α_Ξ , along with the decay parameter of the charge-conjugated process $\Xi^+ \rightarrow \bar{\Lambda}\pi^+$ denoted as $\bar{\alpha}_\Xi$, can be used to define the CP observable A_{CP}^Ξ . The dominant transition in such processes is $\Delta I = 1/2$ [12, 15]. At leading order,

$$A_{CP} = \frac{\alpha + \bar{\alpha}}{\alpha - \bar{\alpha}} = -\tan(\delta_P - \delta_S) \tan(\xi_P - \xi_S). \quad (1)$$

The strong phase difference $(\delta_P - \delta_S)$ signifies the final-state interaction between the daughter baryon and pion, while the weak phase difference, $(\xi_P - \xi_S)$, denotes the strength of the CP violation contribution. Since the strong phases are small [12, 16], any CP violation in A_{CP}^Ξ would be suppressed. However, with ϕ_Ξ and its charge conjugate, $\bar{\phi}_\Xi$, it becomes possible to disentangle and determine both the strong and weak phase differences via

$$(\delta_P - \delta_S)_{\Delta I} = \frac{\sqrt{1 - \langle \alpha_\Xi \rangle^2}}{\langle \alpha_\Xi \rangle} \langle \phi_\Xi \rangle, \quad (2)$$

$$(\xi_P - \xi_S)_{\Delta I} = \frac{\sqrt{1 - \langle \alpha_\Xi \rangle^2}}{\langle \alpha_\Xi \rangle} \Delta\phi_{CP}^\Xi. \quad (3)$$

Here $\langle \alpha_\Xi \rangle$ and $\langle \phi_\Xi \rangle$ are the average values, $\langle \alpha_\Xi \rangle = (\alpha_\Xi - \bar{\alpha}_\Xi)/2$ and $\langle \phi_\Xi \rangle = (\phi_\Xi - \bar{\phi}_\Xi)/2$, respectively. The variable $\Delta\phi_{CP}^\Xi = (\phi_\Xi + \bar{\phi}_\Xi)/2$ is the second CP observable, which can be determined experimentally. In particular, the weak phase differences in hyperon $\Delta S = 1$ decays are related to the ϵ'/ϵ parameter determined from kaon decays. A general theoretical framework can be constructed to relate potential contributions beyond the SM (BSM), represented by chromomagnetic-penguin operators, across the observables of both hyperon and kaon decays. This formal connection enables a consistent analysis of new physics effects in these distinct but related decay processes. Currently, the constraints are still set by the kaon data which gives the upper limit of the BSM contribution as $(\xi_P - \xi_S)_{\text{BSM}} \leq 3.7 \times 10^{-3}$ rad for the $\Xi \rightarrow \Lambda\pi$ decay [11, 12].

To determine the weak phase difference from a single weak decay chain $\Xi^- \rightarrow \Lambda(\rightarrow p\pi^-)\pi^-$, the Ξ^- and Ξ^+ must be significantly polarized. Alternatively, if the $\Xi^-\bar{\Xi}^+$ pairs are produced in a spin-entangled system, as they are for $J/\psi \rightarrow \Xi^-\bar{\Xi}^+$ decays, the strong and weak phases are accessible from the $\Xi^- - \bar{\Xi}^+$ spin correlations [16, 17]. This method was first implemented for the study of $J/\psi \rightarrow \Xi^-\bar{\Xi}^+$ decays by the BESIII collaboration, based on 1.3×10^9 J/ψ events, where the weak phase difference was quantified as $(\xi_P - \xi_S) = (1.2 \pm 3.4 \pm 0.8) \times 10^{-2}$ rad [16]. Subsequent determinations of the weak phase difference with BESIII for the $J/\psi \rightarrow \Xi^0(\rightarrow \Lambda(\rightarrow p\pi^-)\pi^0)\bar{\Xi}^0(\rightarrow \bar{\Lambda}(\rightarrow \bar{p}\pi^+)\pi^0)$ [18] and $J/\psi \rightarrow \Xi^-(\rightarrow \Lambda(\rightarrow p\pi^-)\pi^-)\bar{\Xi}^+(\rightarrow \bar{\Lambda}(\rightarrow \bar{n}\pi^0)\pi^+)$ [15] processes were performed with the same formalism.

For all these measurements, the strong phase differences were found to be compatible with zero. This stands in contrast to the latest theoretical estimate, $(15.4 \pm 0.3) \times 10^{-2}$ rad [19], and to the single non-BESIII experimental result $(10.2 \pm 3.9) \times 10^{-2}$ rad, obtained by the Fermilab-based HyperCP experiment [20] combined with $\alpha_\Xi = -0.376$ [16, 21]. The available theoretical predictions of the strong phase difference use different models, such as the N/D method [22], the baryon chiral perturbative theory [19, 23–29], or the relativistic chiral unitary approach [30–33]. However, current theoretical frameworks are still unable to reliably predict the strong phase difference of $\Xi^- \rightarrow \Lambda\pi^-$. Here, the experimental results serve as a guide for the theoretical community.

In this Letter, we present the most precise determination of the strong and weak phase differences for the Ξ^- hyperon decay. This is done for the $\Xi^- \rightarrow \Lambda\pi^-$ decay based on $(10,087 \pm 44) \times 10^6$ J/ψ events collected by the BESIII experiment [34]. This dataset is approximately eight times larger than the original measurement [16]. The design and performance of the BESIII detector are described in Refs. [35–37]. The simulated Monte Carlo (MC) samples are produced with a GEANT4-based software package [38], which includes the geometric description of the BESIII detector and the detector response. Furthermore, the simulation models the beam energy spread and initial state radiation in the e^+e^- annihilations with generator KKMC [39].

A sample of signal MC events for the process $J/\psi \rightarrow \Xi^-\bar{\Xi}^+$ is used to determine detection efficiencies and optimize event selection criteria. The parameters of the angular distribution in signal MC sample are obtained from the previous measurements [16]. To determine the normalization factors in the maximum likelihood fit, an exclusive MC sample is generated uniformly in phase space. To reduce the discrepancies between the experimental data and MC simulation and to minimize systematic uncertainties due to simulation limits, a control sample of $J/\psi \rightarrow \Xi^-\bar{\Xi}^+$ where only one hyperon is reconstructed is used to estimate differences in hyperon reconstruction and event selection. This estimated discrepancy is taken into account by a weighting factor f , which is correlated to the angular distribution $(\cos\theta_\Xi)$, of the events in the simulated sample, where θ_Ξ is the Ξ^- scattering angle with respect to the e^+ beam in the e^+e^- center-of-mass system. An *inclusive* MC sample is produced to estimate backgrounds. This sample includes the production of the J/ψ resonance and the continuum processes incorporated in KKMC [39]. It also includes the subsequent J/ψ particle decays, modeled with EVTGEN [40] using branching fractions from the Particle Data Group (PDG) [41], when available or otherwise estimated with LUNDCHARM [42].

The final event sample is obtained by a full reconstruction of the $\Xi^-\bar{\Xi}^+ \rightarrow \Lambda\pi^-\bar{\Lambda}\pi^+ \rightarrow p\pi^-\pi^-\bar{p}\pi^+\pi^+$ process. For this purpose, at least three positively and three negatively charged tracks are required, where all tracks must fulfill the multilayer drift chamber (MDC) re-

construction requirement $|\cos\theta_{\text{LAB}}| < 0.93$, where θ_{LAB} is the polar angle relative to the positron beam direction. From this subset, the $\Xi^- (\bar{\Xi}^+)$ candidates are reconstructed using two negative (positive) and one positive (negative) charged tracks. The two Ξ decay chains are reconstructed separately, and are described here for the sequence $\Xi^- \rightarrow \Lambda\pi^- \rightarrow p\pi^-\pi^-$. To select the candidate Ξ^- , one proton and two π^- mesons must be identified. Events containing candidate protons with momenta larger than 0.3 GeV/c or pions with momenta less than 0.3 GeV/c are selected, which corresponds to non-overlapping momentum distributions of protons and pions of the signal process. The Λ and Ξ^- particles are reconstructed from vertex fits by first combining the $p\pi_i^-$ pair to a Λ and then the $\Lambda\pi_j^-$ ($i \neq j$) pair to a Ξ^- candidate. The fits take into account the nonzero flight paths of the hyperons, which can give rise to different production and decay positions. The remaining candidates are then required to pass additional kinematic constraints to reject non- Λ , non- Ξ and combinatorial background contributions with $\delta < 0.016$ GeV/c², where

$$\delta = \sqrt{(m_{\Lambda\pi^-} - m_{\Xi^-})^2 + R^2(m_{p\pi^-} - m_{\Lambda})^2}. \quad (4)$$

Here the m_{Ξ^-} and m_{Λ} are the PDG masses [41] and $m_{\Lambda\pi^-}$ ($m_{p\pi^-}$) is the invariant mass of the $\Lambda\pi^-$ ($p\pi^-$) combination. The $R = \sigma_{\Xi^-}/\sigma_{\Lambda}$ is the ratio of the resolution of the $m_{\Lambda\pi^-}$ distribution over that of the $m_{p\pi^-}$ distribution, where the resolution is extracted by fitting the mass distribution with a sum of two Gaussian functions. The selection criterion for δ is validated using a figure of merit (FOM) defined as $S/\sqrt{S+B}$, where S represents the number of signal events estimated from the MC simulation, and B denotes the background contribution. The quantity $S+B$ is derived from data events. Events where the reconstruction algorithm gives a negative decay length reading are rejected. A four-constraint (4C) kinematic fit requiring energy and momentum conservation is imposed on the $e^+e^- \rightarrow J/\psi \rightarrow \Xi^-\bar{\Xi}^+$ system, and only events satisfying the optimized requirement of $\chi_{4C}^2 < 200$ by FOM are retained for further analysis. This kinematic constraint effectively removes background processes with the same charged final-state topology but containing extra neutral particles, and improves hyperon mass resolution.

After applying all aforementioned selection criteria, 5.8×10^5 $e^+e^- \rightarrow \Xi^-\bar{\Xi}^+$ candidates remain in the final sample. The amount of background contamination from this sample is evaluated with a two-dimensional sideband using a looser requirement of $\delta(\bar{\delta})$. Two regions in the distribution $m_{\Lambda\pi^-}$ versus $m_{\bar{\Lambda}\pi^+}$ are selected as the estimation areas for the sidebands where the lower and upper limitations correspond to $1.274 < m_{\Lambda\pi^-} - (m_{\bar{\Lambda}\pi^+}) < 1.306$ GeV/c² and $1.338 < m_{\Lambda\pi^-} - (m_{\bar{\Lambda}\pi^+}) < 1.370$ GeV/c², respectively. The number of sideband background events is found to be 2034 ± 45 , or 0.4%, after normalizing the data events to the range of $\delta(\bar{\delta}) < 0.016$ GeV/c².

The formalism which has been developed to determine the joint angular distribution [16, 43], allows for a di-

rect measurement of the two $J/\psi \rightarrow \Xi^-\bar{\Xi}^+$ production parameters, α_ψ and $\Delta\Phi$, and six weak decay parameters (α_Λ , α_Ξ , ϕ_Ξ) of the $\Xi^- \rightarrow \Lambda\pi^-$, $\Lambda \rightarrow p\pi^-$ and their charge conjugated parameters ($\bar{\alpha}_\Lambda$, $\bar{\alpha}_\Xi$, $\bar{\phi}_\Xi$). These eight parameters are fully determined from the nine helicity angles $\xi = \{\theta_\Xi, \theta_\Lambda, \varphi_\Lambda, \theta_{\bar{\Lambda}}, \varphi_{\bar{\Lambda}}, \theta_p, \varphi_p, \theta_{\bar{p}}, \varphi_{\bar{p}}\}$, where except for θ_Ξ , the other eight parameters are the polar and azimuthal helicity angles of the Λ , $\bar{\Lambda}$, proton and anti-proton, respectively [16, 43]. A maximum log-likelihood fit, following Refs. [16, 44], is used, where the sideband background events are subtracted from the fit. The MC samples are approximately thirty times larger than data to ensure that uncertainties due to MC statistics are sufficiently minimized. To illustrate the fit quality, the transverse polarization and the diagonal spin correlations defined in Ref. [43] are shown in Fig. 2. The fit results are summarized in Table I.

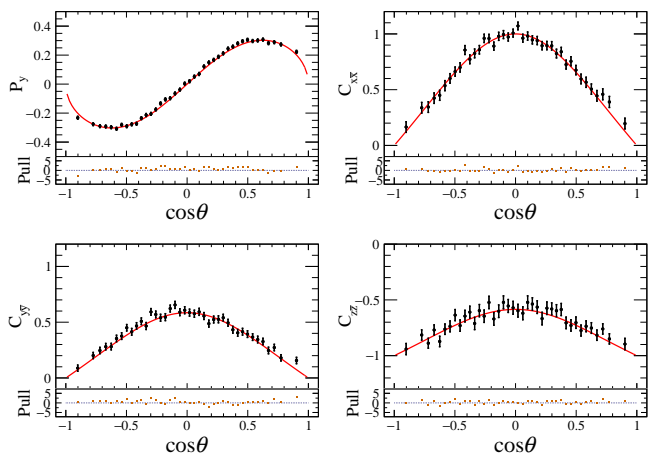


FIG. 2. Acceptance distributions of transverse polarization and spin correlations as a function of $\cos\theta_\Xi$. The black points with error bars show the results from local fits in bins of $\cos\theta_\Xi$, where the error bars represent statistical uncertainties. The red curves correspond to the global fit using the production parameters α_ψ and $\Delta\Phi$.

The event sample is eight times larger than the previous study in Ref. [16], which improves the statistical uncertainty by more than a factor of 2.5. The systematic uncertainties can be divided into two sources. One is from the discrepancy between data and MC simulation, including uncertainties on the Ξ reconstruction and background estimations. The other source comes from the potential bias of the fit method. The systematic uncertainty due to the $\Xi^-\bar{\Xi}^+$ reconstruction includes contributions from track selection, Λ reconstruction, the 4C kinematic fit, Ξ mass window selection and Ξ decay length requirement. It is evaluated using a control sample of $J/\psi \rightarrow \Xi^-\bar{\Xi}^+$, where only one hyperon is reconstructed, and depends on the polar angles θ of Ξ^- and $\bar{\Xi}^+$. By applying Gaussian sampling to the weighting factor referred to as the above f , the maximum likelihood fit is repeated one hundred times. The standard deviation of

TABLE I. Results for the $J/\psi \rightarrow \Xi^- \bar{\Xi}^+$ fitted parameters and CP observables, as well as the comparisons with the previous best measurements. The first and second uncertainties are statistical and systematic, respectively.

Parameter	This work	Previous best result
α_ψ	$0.5851 \pm 0.0044 \pm 0.0034$	$0.611 \pm 0.007^{+0.013}_{-0.007}$ [15]
$\Delta\Phi$ (rad)	$1.2205 \pm 0.0159 \pm 0.0056$	$1.30 \pm 0.03^{+0.02}_{-0.03}$ [15]
α_Ξ	$-0.3813 \pm 0.0026 \pm 0.0005$	$-0.367 \pm 0.004^{+0.003}_{-0.004}$ [15]
$\bar{\alpha}_\Xi$	$0.3873 \pm 0.0026 \pm 0.0006$	$0.374 \pm 0.004^{+0.003}_{-0.004}$ [15]
ϕ_Ξ (rad)	$-0.0008 \pm 0.0072 \pm 0.0010$	$-0.016 \pm 0.012^{+0.004}_{-0.008}$ [15]
$\bar{\phi}_\Xi$ (rad)	$0.0020 \pm 0.0072 \pm 0.0006$	$0.010 \pm 0.012^{+0.003}_{-0.013}$ [15]
α_Λ	$0.7434 \pm 0.0039 \pm 0.0015$	$0.7519 \pm 0.0036 \pm 0.0024$ [45]
$\bar{\alpha}_\Lambda$	$-0.7478 \pm 0.0038 \pm 0.0015$	$-0.7559 \pm 0.0036 \pm 0.0030$ [45]
$(\xi_P - \xi_S) \times 10^{-2}$ (rad)	$-0.2 \pm 1.2 \pm 0.1$	$0.7 \pm 2.0^{+1.8}_{-0.5}$ [15]
$(\delta_P - \delta_S) \times 10^{-2}$ (rad)	$0.3 \pm 1.2 \pm 0.2$	$3.3 \pm 2.0^{+0.8}_{-1.2}$ [15]
$A_{CP}^\Xi \times 10^{-3}$	$-7.8 \pm 4.8 \pm 0.8$	$-9 \pm 8^{+7}_{-2}$ [15]
$\Delta\phi_{CP}^\Xi \times 10^{-3}$ (rad)	$0.6 \pm 5.1 \pm 0.2$	$-3 \pm 8^{+3}_{-7}$ [15]
$A_{CP}^\Lambda \times 10^{-3}$	$-2.9 \pm 4.3 \pm 0.7$	$-2.5 \pm 4.6 \pm 1.2$ [45]
$\langle\alpha_\Xi\rangle$	$-0.3843 \pm 0.0018 \pm 0.0005$	$-0.373 \pm 0.005 \pm 0.002$ [16]
$\langle\phi_\Xi\rangle$ (rad)	$-0.0014 \pm 0.0050 \pm 0.0008$	$0.016 \pm 0.014 \pm 0.007$ [16]
$\langle\alpha_\Lambda\rangle$	$0.7456 \pm 0.0022 \pm 0.0014$	$0.7542 \pm 0.0010 \pm 0.0024$ [45]

TABLE II. Absolute values of systematic uncertainties on the measurements of the fitted parameters in the $J/\psi \rightarrow \Xi^- \bar{\Xi}^+$ process. All entries have been multiplied by 10^3 .

Parameter	Fit method	Reconstruction	Background	Total
α_ψ	0.2	3.0	1.6	3.4
$\Delta\Phi$	0.0	4.6	3.3	5.6
α_Ξ	0.3	0.2	0.4	0.5
$\bar{\alpha}_\Xi$	0.3	0.2	0.5	0.6
ϕ_Ξ	0.9	0.1	0.3	1.0
$\bar{\phi}_\Xi$	0.5	0.1	0.3	0.6
α_Λ	0.5	0.3	1.3	1.5
$\bar{\alpha}_\Lambda$	0.5	0.3	1.4	1.5

the fit results, extracted from a Gaussian fit, is taken as the systematic uncertainty. The background estimation uncertainty is assessed by including and excluding the sideband background events. The difference between the two results is assigned as a systematic uncertainty. The fit bias is examined using three hundred pseudo-experiments, generated with input parameters identical to those reported in Ref. [16]. The systematic uncertainty from the fit procedure is taken to be the absolute difference between the input and output values in the pseudo-experiments. All systematic uncertainties are listed in Table II. The total systematic uncertainty is obtained by summing the individual contributions in quadrature.

The $\Xi^- \bar{\Xi}^+$ production and decay parameters of α_ψ , $\Delta\Phi$, α_Ξ , $\bar{\alpha}_\Xi$, ϕ_Ξ , and $\bar{\phi}_\Xi$ are determined with the most accurate statistical and systematic uncertainties available, as shown in Table I and the measured values of these decay parameters are in agreement with previous

results.

The measurement of the average values of $\langle\phi_\Xi\rangle$ and $\langle\alpha_\Xi\rangle$ enable a direct determination of the strong and weak phase differences via Eqs. (2) and (3). Our result on the strong phase difference, $(\delta_P - \delta_S) = (0.3 \pm 1.2 \pm 0.2) \times 10^{-2}$ rad, is consistent with zero within the uncertainties. It is in agreement with the earlier BESIII results, but is different from the HyperCP value by 2.3σ [20], and disfavors the latest theoretical value by 11.8σ [19]. The weak phase difference is determined to be $(\xi_P - \xi_S) = (-0.2 \pm 1.2 \pm 0.1) \times 10^{-2}$ rad. To our knowledge, this is the most precise weak phase determination for any baryon weak decay, but its precision is still two orders of magnitude lower than the corresponding SM prediction $(\xi_P - \xi_S)_{\text{SM}} = -(2.1 \pm 1.7) \times 10^{-4}$ rad [12]. Our results of $(\delta_P - \delta_S)$ and $(\xi_P - \xi_S)$, and the theoretical predictions and the other measurements are shown in Fig. 3.

The extracted $\Xi^- \bar{\Xi}^+$ decay parameters allow for two CP symmetry tests. The asymmetry A_{CP}^Ξ is measured to be $(-7.8 \pm 4.8 \pm 0.8) \times 10^{-3}$. The corresponding SM prediction is $0.5 \times 10^{-5} < A_{CP, \text{SM}}^\Xi < 6 \times 10^{-5}$ [12]. Our result is consistent with the SM prediction within 1.5σ . Another CP test, defined by the parameters ϕ_Ξ and $\bar{\phi}_\Xi$, yields $\Delta\phi_{CP}^\Xi = (0.6 \pm 5.1 \pm 0.2) \times 10^{-3}$ rad. The first and second uncertainties are statistical and systematic, respectively.

The $\Lambda\bar{\Lambda}$ decay parameters α_Λ and $\bar{\alpha}_\Lambda$ are also measured in the $J/\psi \rightarrow \Xi^- \bar{\Xi}^+ \rightarrow \Lambda\bar{\Lambda}\pi^-\pi^+$ decay. Despite being based on a data sample six times smaller, our results are statistically comparable with the results obtained from $J/\psi \rightarrow \Lambda\bar{\Lambda}$ [45], while exhibiting significantly reduced systematic uncertainties. This is explained by the product with α_Λ and spin polarization. The correlation coefficient between the parameters is

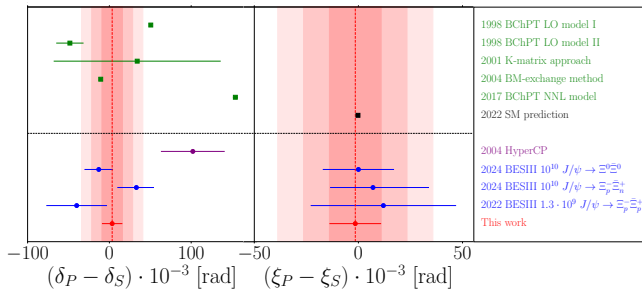


FIG. 3. Strong and weak phase differences in hyperon processes. The red dots with error bars represent the results in this work, which indicate the best results of $(\delta_P - \delta_S)_{\Xi^-}$ and $(\xi_P - \xi_S)_{\Xi^-}$. The blue dots with error bars denote the previous BESIII results from the processes $J/\psi \rightarrow \Xi^- \Xi^+ \rightarrow \Lambda(p\pi^-)\pi^-\bar{\Lambda}(\bar{n}\pi^0)\pi^+$ [15], $J/\psi \rightarrow \Xi^- \Xi^+ \rightarrow \Lambda(p\pi^-)\pi^-\bar{\Lambda}(\bar{p}\pi^+)\pi^+$ [16], and $J/\psi \rightarrow \Xi^0 \Xi^0$ [18], respectively. The purple dot with error bar indicates the result of $(\delta_P - \delta_S)_{\Xi^-}$ measured by the HyperCP collaboration [20]. The black square with error bar implies the predictions from the SM for weak phase difference [12]. The green squares with error bars denote the theoretical predictions on the strong phase differences using various models [19, 24, 25, 27, 29]. The inner, middle, and outer bands represent 68.2%, 95.4%, and 99.7% confidence intervals of variables in this work, respectively.

$\rho(\alpha_\Lambda, \bar{\alpha}_\Lambda)_{J/\psi \rightarrow \Xi^- \Xi^+} = 0.372$, significantly lower than $\rho(\alpha_\Lambda, \bar{\alpha}_\Lambda)_{J/\psi \rightarrow \Lambda \bar{\Lambda}} = 0.850$. This implies that our measurement yields a more precise determination of A_{CP} , but a less precise estimate of the average value of α_Λ . The CP asymmetry of the Λ hyperon is measured to be $A_{CP}^\Lambda = (-2.9 \pm 4.3 \pm 0.7) \times 10^{-3}$ representing the most precise determination to date. The CP violation test reveals no significant deviation from CP symmetry. The average value is determined to be $\langle \alpha_\Lambda \rangle = (\alpha_\Lambda - \bar{\alpha}_\Lambda)/2 = 0.7456 \pm 0.0022 \pm 0.0014$, indicating a discrepancy of 2.3σ compared to the result from $J/\psi \rightarrow \Lambda \bar{\Lambda}$.

In summary, by using $(10,087 \pm 44) \times 10^6$ J/ψ events [34], the most precise measurements of the Ξ strong phase and weak phase differences are determined in the $J/\psi \rightarrow \Xi^- \Xi^+$ decay, as summarized in Table I. Our measurements are consistent with the previous BESIII results of the double-strange hyperon [15, 16, 44], with significantly improved accuracy.

Nonetheless, our results of the strong and weak phase differences in baryon weak decays remain consistent with zero. Probing possible non-zero values would require substantially larger data samples; future facilities such as

the next-generation tau-charm physics facility [12, 46, 47] and PANDA [48] will provide important steps in this direction. The investigation of potential systematic sources put forth by this analysis will be useful for the super tau-charm facility in particular [47], which aims to produce a sample of 10^{12} J/ψ .

ACKNOWLEDGMENTS

Thanks to Jusak Tandean for useful discussions about the theoretical approaches related to the strong phase difference. The BESIII Collaboration thanks the staff of BEPCII (<https://cstr.cn/31109.02.BEPC>) and the IHEP computing center for their strong support. This work is supported in part by National Key R&D Program of China under Contracts Nos. 2023YFA1606000, 2023YFA1606704; National Natural Science Foundation of China (NSFC) under Contracts Nos. 12247101, 11635010, 11935015, 11935016, 11935018, 12025502, 12035009, 12035013, 12061131003, 12192260, 12192261, 12192262, 12192263, 12192264, 12192265, 12221005, 12225509, 12235017, 12361141819; the Fundamental Research Funds for the Central Universities No. lzujbky-2025-ytA05, No. lzujbky-2025-it06, No. lzujbky-2024-jdzz06; the Natural Science Foundation of Gansu Province No. 22JR5RA389, No.25JRRA799; the ‘111 Center’ under Grant No. B20063; Beijing Natural Science Foundation of China (BNSF) under Contract No. IS23014; the Chinese Academy of Sciences (CAS) Large-Scale Scientific Facility Program; the Strategic Priority Research Program of Chinese Academy of Sciences under Contract No. XDA0480600; CAS under Contract No. YSBR-101; 100 Talents Program of CAS; The Institute of Nuclear and Particle Physics (INPAC) and Shanghai Key Laboratory for Particle Physics and Cosmology; ERC under Contract No. 758462; German Research Foundation DFG under Contract No. FOR5327; Istituto Nazionale di Fisica Nucleare, Italy; Knut and Alice Wallenberg Foundation under Contracts Nos. 2021.0174, 2021.0299; Ministry of Development of Turkey under Contract No. DPT2006K-120470; National Research Foundation of Korea under Contract No. NRF-2022R1A2C1092335; National Science and Technology fund of Mongolia; Polish National Science Centre under Contract No. 2024/53/B/ST2/00975; STFC (United Kingdom); Swedish Research Council under Contract No. 2019.04595; the Olle Engkvist Foundation under Contract No. 200-0605; U. S. Department of Energy under Contract No. DE-FG02-05ER41374

-
- [1] A. D. Sakharov, *Pisma Zh. Eksp. Teor. Fiz.* **5**, 32 (1967).
[2] N. Cabibbo, *Phys. Rev. Lett.* **10**, 531 (1963).
[3] M. Kobayashi and T. Maskawa, *Prog. Theor. Phys.* **49**, 652 (1973).
[4] W. Bernreuther, *Lect. Notes Phys.* **591**, 237 (2002),

- arXiv:hep-ph/0205279.
[5] L. Canetti, M. Drewes, and M. Shaposhnikov, *New J. Phys.* **14**, 095012 (2012).
[6] J. H. Christenson, J. W. Cronin, V. L. Fitch, and R. Turlay, *Phys. Rev. Lett.* **13**, 138 (1964).

- [7] B. Aubert *et al.* (BaBar), *Phys. Rev. Lett.* **87**, 091801 (2001).
- [8] K. Abe *et al.* (Belle), *Phys. Rev. Lett.* **87**, 091802 (2001).
- [9] R. Aaij *et al.* (LHCb), *Phys. Rev. Lett.* **122**, 211803 (2019).
- [10] R. Aaij *et al.* (LHCb), *Nature* **643**, 1223 (2025), [arXiv:2503.16954 \[hep-ex\]](#).
- [11] J. Tandean, *Phys. Rev. D* **69**, 076008 (2004).
- [12] N. Salone, P. Adlarson, V. Batzskaya, A. Kupsc, S. Leupold, and J. Tandean, *Phys. Rev. D* **105**, 116022 (2022).
- [13] J. F. Donoghue, X.-G. He, and S. Pakvasa, *Phys. Rev. D* **34**, 833 (1986).
- [14] T. D. Lee and C.-N. Yang, *Phys. Rev.* **108**, 1645 (1957).
- [15] M. Ablikim *et al.* (BESIII), *Phys. Rev. Lett.* **132**, 101801 (2024).
- [16] M. Ablikim *et al.* (BESIII), *Nature* **606**, 64 (2022).
- [17] P. Adlarson and A. Kupsc, *Phys. Rev. D* **100**, 114005 (2019).
- [18] M. Ablikim *et al.* (BESIII), *Phys. Rev. D* **108**, L031106 (2023).
- [19] B.-L. Huang, J.-S. Zhang, Y.-D. Li, and N. Kaiser, *Phys. Rev. D* **96**, 016021 (2017).
- [20] T. Holmstrom *et al.* (HyperCP), *Phys. Rev. Lett.* **93**, 262001 (2004).
- [21] The HyperCP paper determined ϕ_{Ξ} and extracted the strong phase difference from $\alpha_{\Xi}\alpha_{\Lambda}$, relying on the assumed value $\alpha_{\Lambda} = 0.642 \pm 0.013$, which has since been revised by BESIII.
- [22] R. Nath and A. Kumar, *Nuovo Cim.* **36**, 669 (1965).
- [23] M. Lu, M. B. Wise, and M. J. Savage, *Phys. Lett. B* **337**, 133 (1994).
- [24] A. N. Kamal, *Phys. Rev. D* **58**, 077501 (1998).
- [25] A. Datta, P. O'Donnell, and S. Pakvasa, (1998), [arXiv:hep-ph/9806374](#).
- [26] A. Datta and S. Pakvasa, *Phys. Lett. B* **344**, 430–432 (1995).
- [27] J. Tandean, A. W. Thomas, and G. E. Valencia, *Phys. Rev. D* **64**, 014005 (2001).
- [28] N. Kaiser, *Phys. Rev. C* **64**, 045204 (2001), [Erratum: *Phys.Rev.C* 73, 069902 (2006)].
- [29] C. C. Barros, Jr., (2004), [arXiv:hep-ph/0402093](#).
- [30] U.-G. Meissner and J. A. Oller, *Phys. Rev. D* **64**, 014006 (2001).
- [31] J. A. Oller, J. Prades, and M. Verbeni, *Phys. Rev. Lett.* **95**, 172502 (2005).
- [32] J. A. Oller, *Eur. Phys. J. A* **28**, 63 (2006).
- [33] Z.-H. Guo and J. A. Oller, *Phys. Rev. C* **87**, 035202 (2013).
- [34] M. Ablikim *et al.* (BESIII), *Chin. Phys. C* **46**, 074001 (2022).
- [35] M. Ablikim *et al.* (BESIII), *Nucl. Instrum. Meth. A* **614**, 345 (2010).
- [36] J. Z. Bai *et al.* (BES), *Nucl. Instrum. Meth. A* **458**, 627 (2001).
- [37] C. Yu *et al.*, in *7th International Particle Accelerator Conference* (2016) p. TUYA01.
- [38] S. Agostinelli *et al.* (GEANT4), *Nucl. Instrum. Meth. A* **506**, 250 (2003).
- [39] S. Jadach, B. F. L. Ward, and Z. Was, *Phys. Rev. D* **63**, 113009 (2001).
- [40] R.-G. Ping, *Chin. Phys. C* **32**, 599 (2008).
- [41] S. Navas *et al.* (Particle Data Group), *Phys. Rev. D* **110**, 030001 (2024).
- [42] J. C. Chen, G. S. Huang, X. R. Qi, D. H. Zhang, and Y. S. Zhu, *Phys. Rev. D* **62**, 034003 (2000).
- [43] E. Perotti, G. Fäldt, A. Kupsc, S. Leupold, and J. J. Song, *Phys. Rev. D* **99**, 056008 (2019).
- [44] M. Ablikim *et al.* (BESIII), *Phys. Rev. D* **106**, L091101 (2022).
- [45] M. Ablikim *et al.* (BESIII), *Phys. Rev. Lett.* **129**, 131801 (2022).
- [46] A. E. Bondar *et al.* (Charm-Tau Factory), *Phys. Atom. Nucl.* **76**, 1072 (2013).
- [47] M. Achasov *et al.*, *Front. Phys. (Beijing)* **19**, 14701 (2024).
- [48] G. Barucca *et al.* (PANDA), *Eur. Phys. J. A* **57**, 154 (2021).

END MATTER

This End Matter introduces the correlation coefficients of the fit parameters, as shown in Table III, which is helpful for understanding the correlations among the parameters.

TABLE III. Correlation coefficients of the fit results.

	α_{ψ}	$\Delta\Phi$	α_{Ξ}	$\bar{\alpha}_{\Xi}$	ϕ_{Ξ}	$\bar{\phi}_{\Xi}$	α_{Λ}	$\bar{\alpha}_{\Lambda}$
α_{ψ}	1.000	0.394	-0.023	0.016	-0.016	0.017	-0.116	0.107
$\Delta\Phi$		1.000	-0.035	0.021	0.010	-0.002	-0.148	0.135
α_{Ξ}			1.000	0.035	-0.002	0.001	0.312	0.078
$\bar{\alpha}_{\Xi}$				1.000	0.000	-0.001	0.083	0.316
ϕ_{Ξ}					1.000	0.029	0.004	0.001
$\bar{\phi}_{\Xi}$						1.000	0.001	0.006
α_{Λ}							1.000	0.372
$\bar{\alpha}_{\Lambda}$								1.000

M. Ablikim¹ , M. N. Achasov^{4,b} , P. Adlarson⁸¹ , X. C. Ai⁸⁶ , R. Aliberti³⁹ , A. Amoroso^{80A,80C} , Q. An^{77,64,†} , Y. Bai⁶² , O. Bakina⁴⁰ , Y. Ban^{50,g} , H.-R. Bao⁷⁰ , X. L. Bao⁴⁹ , V. Batzskaya^{1,48} , K. Begzsuren³⁵ , N. Berger³⁹ , M. Berlowski⁴⁸ , M. B. Bertani^{30A} , D. Bettoni^{31A} , F. Bianchi^{80A,80C} , E. Bianco^{80A,80C} , A. Bortone^{80A,80C} , I. Boyko⁴⁰ , R. A. Briere⁵ , A. Brueggemann⁷⁴ , H. Cai⁸² , M. H. Cai^{42,j,k} , X. Cai^{1,64} , A. Calcaterra^{30A} , G. F. Cao^{1,70} , N. Cao^{1,70} , S. A. Cetin^{68A} , X. Y. Chai^{50,g} , J. F. Chang^{1,64} , T. T. Chang⁴⁷ , G. R. Che⁴⁷ , Y. Z. Che^{1,64,70} , C. H. Chen¹⁰ , Chao Chen⁶⁰ , G. Chen¹ , H. S. Chen^{1,70} , H. Y. Chen²¹ , M. L. Chen^{1,64,70} , S. J. Chen⁴⁶ , S. M. Chen⁶⁷ , T. Chen^{1,70} , W. Chen⁴⁹ , X. R. Chen^{34,70} , X. T. Chen^{1,70} , X. Y. Chen^{12,f} , Y. B. Chen^{1,64} , Y. Q. Chen¹⁶ , Z. K. Chen⁶⁵ , J. Cheng⁴⁹ , L. N. Cheng⁴⁷ , S. K. Choi¹¹ , X. Chu^{12,f} , G. Cibinetto^{31A} , F. Cossio^{80C} , J. Cottee-Meldrum⁶⁹ , H. L. Dai^{1,64} , J. P. Dai⁸⁴ , X. C. Dai⁶⁷ , A. Dbeyssi¹⁹ , R. E. de Boer³ , D. Dedovich⁴⁰ , C. Q. Deng⁷⁸ , Z. Y. Deng¹ , A. Denig³⁹ , I. Denisenko⁴⁰ , M. Destefanis^{80A,80C} , F. De Mori^{80A,80C} , X. X. Ding^{50,g} , Y. Ding⁴⁴ , Y. X. Ding³² , J. Dong^{1,64}

L. Y. Dong^{1,70} , M. Y. Dong^{1,64,70} , X. Dong⁸² , M. C. Du¹ , S. X. Du⁸⁶ , S. X. Du^{12,f} , X. L. Du⁸⁶ ,
 Y. Y. Duan⁶⁰ , Z. H. Duan⁴⁶ , P. Egorov^{40,a} , G. F. Fan⁴⁶ , J. J. Fan²⁰ , Y. H. Fan⁴⁹ , J. Fang^{1,64} , J. Fang⁶⁵ ,
 S. S. Fang^{1,70} , W. X. Fang¹ , Y. Q. Fang^{1,64,i} , L. Fava^{80B,80C} , F. Feldbauer³ , G. Felici^{30A} , C. Q. Feng^{77,64} ,
 J. H. Feng¹⁶ , L. Feng^{42,j,k} , Q. X. Feng^{42,j,k} , Y. T. Feng^{77,64} , M. Fritsch³ , C. D. Fu¹ , J. L. Fu⁷⁰ ,
 Y. W. Fu^{1,70} , H. Gao⁷⁰ , Y. Gao^{77,64} , Y. N. Gao^{50,g} , Y. N. Gao²⁰ , Y. Y. Gao³² , Z. Gao⁴⁷ ,
 S. Garbolino^{80C} , I. Garzia^{31A,31B} , L. Ge⁶² , P. T. Ge²⁰ , Z. W. Ge⁴⁶ , C. Geng⁶⁵ , E. M. Gersabeck⁷³ ,
 A. Gilman⁷⁵ , K. Goetzen¹³ , J. Gollub³ , J. D. Gong³⁸ , L. Gong⁴⁴ , W. X. Gong^{1,64} , W. Gradl³⁹ ,
 S. Gramigna^{31A,31B} , M. Greco^{80A,80C} , M. D. Gu⁵⁵ , M. H. Gu^{1,64} , C. Y. Guan^{1,70} , A. Q. Guo³⁴ ,
 J. N. Guo^{12,f} , L. B. Guo⁴⁵ , M. J. Guo⁵⁴ , R. P. Guo⁵³ , X. Guo⁵⁴ , Y. P. Guo^{12,f} , A. Guskov^{40,a} ,
 J. Gutierrez²⁹ , T. T. Han¹ , F. Hanisch³ , K. D. Hao^{77,64} , X. Q. Hao²⁰ , F. A. Harris⁷¹ , C. Z. He^{50,g} ,
 K. L. He^{1,70} , F. H. Heinsius³ , C. H. Heinz³⁹ , Y. K. Heng^{1,64,70} , C. Herold⁶⁶ , P. C. Hong³⁸ , G. Y. Hou^{1,70} ,
 X. T. Hou^{1,70} , Y. R. Hou⁷⁰ , Z. L. Hou¹ , H. M. Hu^{1,70} , J. F. Hu^{61,i} , Q. P. Hu^{77,64} , S. L. Hu^{12,f} ,
 T. Hu^{1,64,70} , Y. Hu¹ , Z. M. Hu⁶⁵ , G. S. Huang^{77,64} , K. X. Huang⁶⁵ , L. Q. Huang^{34,70} , P. Huang⁴⁶ ,
 X. T. Huang⁵⁴ , Y. P. Huang¹ , Y. S. Huang⁶⁵ , T. Hussain⁷⁹ , N. Hüskens³⁹ , N. in der Wiesche⁷⁴ , J. Jackson²⁹ ,
 Q. Ji¹ , Q. P. Ji²⁰ , W. Ji^{1,70} , X. B. Ji^{1,70} , X. L. Ji^{1,64} , X. Q. Jia⁵⁴ , Z. K. Jia^{77,64} , D. Jiang^{1,70} ,
 H. B. Jiang⁸² , P. C. Jiang^{50,g} , S. J. Jiang¹⁰ , M. S. Jiang^{1,64,70} , Y. Jiang⁷⁰ , J. B. Jiao⁵⁴ , J. K. Jiao³⁸ ,
 Z. Jiao²⁵ , L. C. L. Jin¹ , S. Jin⁴⁶ , Y. Jin⁷² , M. Q. Jing^{1,70} , X. M. Jing⁷⁰ , T. Johansson⁸¹ , S. Kabana³⁶ ,
 X. L. Kang¹⁰ , X. S. Kang⁴⁴ , B. C. Ke⁸⁶ , V. Khachatryan²⁹ , A. Khokkaz⁷⁴ , O. B. Kolcu^{68A} , B. Kopf³ ,
 L. Kröger⁷⁴ , M. Kuessner³ , X. Kui^{1,70} , N. Kumar²⁸ , A. Kupsc^{48,81} , W. Kühn⁴¹ , Q. Lan⁷⁸ , W. N. Lan²⁰ ,
 T. T. Lei^{77,64} , M. Lellmann³⁹ , T. Lenz³⁹ , C. Li⁵¹ , C. Li⁴⁷ , C. H. Li⁴⁵ , C. K. Li²¹ , D. M. Li⁸⁶ , F. Li^{1,64} ,
 G. Li¹ , H. B. Li^{1,70} , H. J. Li²⁰ , H. L. Li⁸⁶ , H. N. Li^{61,i} , Hui Li⁴⁷ , J. R. Li⁶⁷ , J. S. Li⁶⁵ , J. W. Li⁵⁴ ,
 K. Li¹ , K. L. Li^{42,j,k} , L. J. Li^{1,70} , Lei Li⁵² , M. H. Li⁴⁷ , M. R. Li^{1,70} , P. L. Li⁷⁰ , P. R. Li^{42,j,k} ,
 Q. M. Li^{1,70} , Q. X. Li⁵⁴ , R. Li^{18,34} , S. X. Li¹² , Shanshan Li^{27,h} , T. Li⁵⁴ , T. Y. Li⁴⁷ , W. D. Li^{1,70} ,
 W. G. Li^{1,i} , X. Li^{1,70} , X. H. Li^{50,g} , X. K. Li⁵⁴ , X. L. Li^{1,9} , X. Z. Li⁶⁵ , Y. Li²⁰ , Y. G. Li⁷⁰ ,
 Y. P. Li³⁸ , Z. H. Li⁴² , Z. J. Li⁶⁵ , Z. X. Li⁴⁷ , Z. Y. Li⁸⁴ , C. Liang⁴⁶ , H. Liang^{77,64} , Y. F. Liang⁵⁹ ,
 Y. T. Liang^{34,70} , G. R. Liao¹⁴ , L. B. Liao⁶⁵ , M. H. Liao⁶⁵ , Y. P. Liao^{1,70} , J. Libby²⁸ , A. Limphirat⁶⁶ ,
 D. X. Lin^{34,70} , L. Q. Lin⁴³ , T. Lin¹ , B. J. Liu¹ , B. X. Liu⁸² , C. X. Liu¹ , F. Liu¹ , F. H. Liu⁵⁸ ,
 Feng Liu⁶ , G. M. Liu^{61,i} , H. Liu^{42,j,k} , H. B. Liu¹⁵ , H. M. Liu^{1,70} , Huihui Liu²² , J. B. Liu^{77,64} , J. J. Liu²¹ ,
 K. Liu^{42,j,k} , K. Liu⁷⁸ , K. Y. Liu⁴⁴ , Ke Liu²³ , L. Liu⁴² , Liang Liu^{77,64} , L. C. Liu⁴⁷ , Lu Liu⁴⁷ ,
 M. H. Liu³⁸ , P. L. Liu¹ , Q. Liu⁷⁰ , S. B. Liu^{77,64} , W. M. Liu^{77,64} , W. T. Liu⁴³ , X. Liu^{42,j,k} , X. K. Liu^{42,j,k} ,
 X. L. Liu^{12,f} , X. Y. Liu⁸² , Y. Liu^{42,j,k} , Y. Liu⁸⁶ , Y. B. Liu⁴⁷ , Z. A. Liu^{1,64,70} , Z. D. Liu¹⁰ , Z. Q. Liu⁵⁴ ,
 Z. Y. Liu⁴² , X. C. Lou^{1,64,70} , H. J. Lu²⁵ , J. G. Lu^{1,64} , X. L. Lu¹⁶ , Y. Lu⁷ , Y. H. Lu^{1,70} , Y. P. Lu^{1,64} ,
 Z. H. Lu^{1,70} , C. L. Luo⁴⁵ , J. R. Luo⁶⁵ , J. S. Luo^{1,70} , M. X. Luo⁸⁵ , T. Luo^{12,f} , X. L. Luo^{1,64} , Z. Y. Lv²³ ,
 X. R. Lyu^{70,n} , Y. F. Lyu⁴⁷ , Y. H. Lyu⁸⁶ , F. C. Ma⁴⁴ , H. L. Ma¹ , Heng Ma^{27,h} , J. L. Ma^{1,70} , L. L. Ma⁵⁴ ,
 L. R. Ma⁷² , Q. M. Ma¹ , R. Q. Ma^{1,70} , R. Y. Ma²⁰ , T. Ma^{77,64} , X. T. Ma^{1,70} , X. Y. Ma^{1,64} , Y. M. Ma³⁴ ,
 F. E. Maas¹⁹ , I. MacKay⁷⁵ , M. Maggiora^{80A,80C} , S. Malde⁷⁵ , Q. A. Malik⁷⁹ , H. X. Mao^{42,j,k} , Y. J. Mao^{50,g} ,
 Z. P. Mao¹ , S. Marcelllo^{80A,80C} , A. Marshall⁶⁹ , F. M. Melendi^{31A,31B} , Y. H. Meng⁷⁰ , Z. X. Meng⁷² ,
 G. Mezzadri^{31A} , H. Miao^{1,70} , T. J. Min⁴⁶ , R. E. Mitchell²⁹ , X. H. Mo^{1,64,70} , B. Moses²⁹ , N. Yu. Muchnoi^{4,b} ,
 J. Muskalla³⁹ , Y. Nefedov⁴⁰

Y. L. Xiao^{12,f} , Z. J. Xiao⁴⁵ , C. Xie⁴⁶ , K. J. Xie^{1,70} , Y. Xie⁵⁴ , Y. G. Xie^{1,64} , Y. H. Xie⁶ , Z. P. Xie^{77,64} ,
T. Y. Xing^{1,70} , D. B. Xiong¹ , C. J. Xu⁶⁵ , G. F. Xu¹ , H. Y. Xu² , M. Xu^{77,64} , Q. J. Xu¹⁷ , Q. N. Xu³² ,
T. D. Xu⁷⁸ , X. P. Xu⁶⁰ , Y. Xu^{12,f} , Y. C. Xu⁸³ , Z. S. Xu⁷⁰ , F. Yan²⁴ , L. Yan^{12,f} , W. B. Yan^{77,64} ,
W. C. Yan⁸⁶ , W. H. Yan⁶ , W. P. Yan²⁰ , X. Q. Yan^{12,f} , Y. Y. Yan⁶⁶ , H. J. Yang^{56,e} , H. L. Yang³⁸ ,
H. X. Yang¹ , J. H. Yang⁴⁶ , R. J. Yang²⁰ , Y. Yang^{12,f} , Y. H. Yang⁴⁶ , Y. Q. Yang¹⁰ , Y. Z. Yang²⁰ ,
Z. P. Yao⁵⁴ , M. Ye^{1,64} , M. H. Ye^{9,i} , Z. J. Ye^{61,i} , Junhao Yin⁴⁷ , Z. Y. You⁶⁵ , B. X. Yu^{1,64,70} , C. X. Yu⁴⁷ ,
G. Yu¹³ , J. S. Yu^{27,h} , L. W. Yu^{12,f} , T. Yu⁷⁸ , X. D. Yu^{50,g} , Y. C. Yu⁸⁶ , Y. C. Yu⁴² , C. Z. Yuan^{1,70} ,
H. Yuan^{1,70} , J. Yuan³⁸ , J. Yuan⁴⁹ , L. Yuan² , M. K. Yuan^{12,f} , S. H. Yuan⁷⁸ , Y. Yuan^{1,70} , C. X. Yue⁴³ ,
Ying Yue²⁰ , A. A. Zafar⁷⁹ , F. R. Zeng⁵⁴ , S. H. Zeng⁶⁹ , X. Zeng^{12,f} , Y. J. Zeng⁶⁵ , Y. J. Zeng^{1,70} ,
Y. C. Zhai⁵⁴ , Y. H. Zhan⁶⁵ , S. N. Zhang⁷⁵ , B. L. Zhang^{1,70} , B. X. Zhang^{1,†} , D. H. Zhang⁴⁷ , G. Y. Zhang²⁰ ,
G. Y. Zhang^{1,70} , H. Zhang^{77,64} , H. Zhang⁸⁶ , H. C. Zhang^{1,64,70} , H. H. Zhang⁶⁵ , H. Q. Zhang^{1,64,70} ,
H. R. Zhang^{77,64} , H. Y. Zhang^{1,64} , J. Zhang⁶⁵ , J. J. Zhang⁵⁷ , J. L. Zhang²¹ , J. Q. Zhang⁴⁵ , J. S. Zhang^{12,f} ,
J. W. Zhang^{1,64,70} , J. X. Zhang^{42,j,k} , J. Y. Zhang¹ , J. Z. Zhang^{1,70} , Jianyu Zhang⁷⁰ , L. M. Zhang⁶⁷ ,
Lei Zhang⁴⁶ , N. Zhang³⁸ , P. Zhang^{1,9} , Q. Zhang²⁰ , Q. Y. Zhang³⁸ , R. Y. Zhang^{42,j,k} , S. H. Zhang^{1,70} ,
Shulei Zhang^{27,h} , X. M. Zhang¹ , X. Y. Zhang⁵⁴ , Y. Zhang¹ , Y. Zhang⁷⁸ , Y. T. Zhang⁸⁶ , Y. H. Zhang^{1,64} ,
Y. P. Zhang^{77,64} , Z. D. Zhang¹ , Z. H. Zhang¹ , Z. L. Zhang³⁸ , Z. L. Zhang⁶⁰ , Z. X. Zhang²⁰ , Z. Y. Zhang⁸² ,
Z. Y. Zhang⁴⁷ , Z. Y. Zhang⁴⁹ , Zh. Zh. Zhang²⁰ , G. Zhao¹ , J. Y. Zhao^{1,70} , J. Z. Zhao^{1,64} , L. Zhao¹ ,
L. Zhao^{77,64} , M. G. Zhao⁴⁷ , S. J. Zhao⁸⁶ , Y. B. Zhao^{1,64} , Y. L. Zhao⁶⁰ , Y. P. Zhao⁴⁹ , Y. X. Zhao^{34,70} ,
Z. G. Zhao^{77,64} , A. Zhemchugov^{40,a} , B. Zheng⁷⁸ , B. M. Zheng³⁸ , J. P. Zheng^{1,64} , W. J. Zheng^{1,70} ,
X. R. Zheng²⁰ , Y. H. Zheng^{70,n} , B. Zhong⁴⁵ , C. Zhong²⁰ , H. Zhou^{39,54,m} , J. Q. Zhou³⁸ , S. Zhou⁶ ,
X. Zhou⁸² , X. K. Zhou⁶ , X. R. Zhou^{77,64} , X. Y. Zhou⁴³ , Y. X. Zhou⁸³ , Y. Z. Zhou^{12,f} , A. N. Zhu⁷⁰ ,
J. Zhu⁴⁷ , K. Zhu¹ , K. J. Zhu^{1,64,70} , K. S. Zhu^{12,f} , L. X. Zhu⁷⁰ , Lin Zhu²⁰ , S. H. Zhu⁷⁶ , T. J. Zhu^{12,f} ,
W. D. Zhu^{12,f} , W. J. Zhu¹ , W. Z. Zhu²⁰ , Y. C. Zhu^{77,64} , Z. A. Zhu^{1,70} , X. Y. Zhuang⁴⁷ , J. H. Zou¹ 

(BESIII Collaboration)

¹ Institute of High Energy Physics, Beijing 100049, People's Republic of China

² Beihang University, Beijing 100191, People's Republic of China

³ Bochum Ruhr-University, D-44780 Bochum, Germany

⁴ Budker Institute of Nuclear Physics SB RAS (BINP), Novosibirsk 630090, Russia

⁵ Carnegie Mellon University, Pittsburgh, Pennsylvania 15213, USA

⁶ Central China Normal University, Wuhan 430079, People's Republic of China

⁷ Central South University, Changsha 410083, People's Republic of China

⁸ Chengdu University of Technology, Chengdu 610059, People's Republic of China

⁹ China Center of Advanced Science and Technology, Beijing 100190, People's Republic of China

¹⁰ China University of Geosciences, Wuhan 430074, People's Republic of China

¹¹ Chung-Ang University, Seoul, 06974, Republic of Korea

¹² Fudan University, Shanghai 200433, People's Republic of China

¹³ GSI Helmholtzcentre for Heavy Ion Research GmbH, D-64291 Darmstadt, Germany

¹⁴ Guangxi Normal University, Guilin 541004, People's Republic of China

¹⁵ Guangxi University, Nanning 530004, People's Republic of China

¹⁶ Guangxi University of Science and Technology, Liuzhou 545006, People's Republic of China

¹⁷ Hangzhou Normal University, Hangzhou 310036, People's Republic of China

¹⁸ Hebei University, Baoding 071002, People's Republic of China

¹⁹ Helmholtz Institute Mainz, Staudinger Weg 18, D-55099 Mainz, Germany

²⁰ Henan Normal University, Xinxiang 453007, People's Republic of China

²¹ Henan University, Kaifeng 475004, People's Republic of China

²² Henan University of Science and Technology, Luoyang 471003, People's Republic of China

²³ Henan University of Technology, Zhengzhou 450001, People's Republic of China

²⁴ Hengyang Normal University, Hengyang 421001, People's Republic of China

²⁵ Huangshan College, Huangshan 245000, People's Republic of China

²⁶ Hunan Normal University, Changsha 410081, People's Republic of China

²⁷ Hunan University, Changsha 410082, People's Republic of China

²⁸ Indian Institute of Technology Madras, Chennai 600036, India

²⁹ Indiana University, Bloomington, Indiana 47405, USA

³⁰ INFN Laboratori Nazionali di Frascati, (A)INFN Laboratori Nazionali di Frascati, I-00044, Frascati, Italy; (B)INFN Sezione di Perugia, I-06100, Perugia, Italy; (C)University of Perugia, I-06100, Perugia, Italy

³¹ INFN Sezione di Ferrara, (A)INFN Sezione di Ferrara, I-44122, Ferrara, Italy; (B)University of Ferrara, I-44122, Ferrara, Italy

³² Inner Mongolia University, Hohhot 010021, People's Republic of China

³³ Institute of Business Administration, University Road, Karachi, 75270 Pakistan

³⁴ Institute of Modern Physics, Lanzhou 730000, People's Republic of China

³⁵ Institute of Physics and Technology, Mongolian Academy of Sciences, Peace Avenue 54B, Ulaanbaatar 13330, Mongolia

³⁶ Instituto de Alta Investigación, Universidad de Tarapacá, Casilla 7D, Arica 1000000, Chile

- ³⁷ Jiangsu Ocean University, Lianyungang 222000, People's Republic of China
- ³⁸ Jilin University, Changchun 130012, People's Republic of China
- ³⁹ Johannes Gutenberg University of Mainz, Johann-Joachim-Becher-Weg 45, D-55099 Mainz, Germany
- ⁴⁰ Joint Institute for Nuclear Research, 141980 Dubna, Moscow region, Russia
- ⁴¹ Justus-Liebig-Universitaet Giessen, II. Physikalisches Institut, Heinrich-Buff-Ring 16, D-35392 Giessen, Germany
- ⁴² Lanzhou University, Lanzhou 730000, People's Republic of China
- ⁴³ Liaoning Normal University, Dalian 116029, People's Republic of China
- ⁴⁴ Liaoning University, Shenyang 110036, People's Republic of China
- ⁴⁵ Nanjing Normal University, Nanjing 210023, People's Republic of China
- ⁴⁶ Nanjing University, Nanjing 210093, People's Republic of China
- ⁴⁷ Nankai University, Tianjin 300071, People's Republic of China
- ⁴⁸ National Centre for Nuclear Research, Warsaw 02-093, Poland
- ⁴⁹ North China Electric Power University, Beijing 102206, People's Republic of China
- ⁵⁰ Peking University, Beijing 100871, People's Republic of China
- ⁵¹ Qufu Normal University, Qufu 273165, People's Republic of China
- ⁵² Renmin University of China, Beijing 100872, People's Republic of China
- ⁵³ Shandong Normal University, Jinan 250014, People's Republic of China
- ⁵⁴ Shandong University, Jinan 250100, People's Republic of China
- ⁵⁵ Shandong University of Technology, Zibo 255000, People's Republic of China
- ⁵⁶ Shanghai Jiao Tong University, Shanghai 200240, People's Republic of China
- ⁵⁷ Shanxi Normal University, Linfen 041004, People's Republic of China
- ⁵⁸ Shanxi University, Taiyuan 030006, People's Republic of China
- ⁵⁹ Sichuan University, Chengdu 610064, People's Republic of China
- ⁶⁰ Soochow University, Suzhou 215006, People's Republic of China
- ⁶¹ South China Normal University, Guangzhou 510006, People's Republic of China
- ⁶² Southeast University, Nanjing 211100, People's Republic of China
- ⁶³ Southwest University of Science and Technology, Mianyang 621010, People's Republic of China
- ⁶⁴ State Key Laboratory of Particle Detection and Electronics, Beijing 100049, Hefei 230026, People's Republic of China
- ⁶⁵ Sun Yat-Sen University, Guangzhou 510275, People's Republic of China
- ⁶⁶ Suranaree University of Technology, University Avenue 111, Nakhon Ratchasima 30000, Thailand
- ⁶⁷ Tsinghua University, Beijing 100084, People's Republic of China
- ⁶⁸ Turkish Accelerator Center Particle Factory Group, (A)Istinye University, 34010, Istanbul, Turkey; (B)Near East University, Nicosia, North Cyprus, 99138, Mersin 10, Turkey
- ⁶⁹ University of Bristol, H H Wills Physics Laboratory, Tyndall Avenue, Bristol, BS8 1TL, UK
- ⁷⁰ University of Chinese Academy of Sciences, Beijing 100049, People's Republic of China
- ⁷¹ University of Hawaii, Honolulu, Hawaii 96822, USA
- ⁷² University of Jinan, Jinan 250022, People's Republic of China
- ⁷³ University of Manchester, Oxford Road, Manchester, M13 9PL, United Kingdom
- ⁷⁴ University of Muenster, Wilhelm-Klemm-Strasse 9, 48149 Muenster, Germany
- ⁷⁵ University of Oxford, Keble Road, Oxford OX13RH, United Kingdom
- ⁷⁶ University of Science and Technology Liaoning, Anshan 114051, People's Republic of China
- ⁷⁷ University of Science and Technology of China, Hefei 230026, People's Republic of China
- ⁷⁸ University of South China, Hengyang 421001, People's Republic of China
- ⁷⁹ University of the Punjab, Lahore-54590, Pakistan
- ⁸⁰ University of Turin and INFN, (A)University of Turin, I-10125, Turin, Italy; (B)University of Eastern Piedmont, I-15121, Alessandria, Italy; (C)INFN, I-10125, Turin, Italy
- ⁸¹ Uppsala University, Box 516, SE-75120 Uppsala, Sweden
- ⁸² Wuhan University, Wuhan 430072, People's Republic of China
- ⁸³ Yantai University, Yantai 264005, People's Republic of China
- ⁸⁴ Yunnan University, Kunming 650500, People's Republic of China
- ⁸⁵ Zhejiang University, Hangzhou 310027, People's Republic of China
- ⁸⁶ Zhengzhou University, Zhengzhou 450001, People's Republic of China

† Deceased

^a Also at the Moscow Institute of Physics and Technology, Moscow 141700, Russia

^b Also at the Novosibirsk State University, Novosibirsk, 630090, Russia

^c Also at the NRC "Kurchatov Institute", PNPI, 188300, Gatchina, Russia

^d Also at Goethe University Frankfurt, 60323 Frankfurt am Main, Germany

^e Also at Key Laboratory for Particle Physics, Astrophysics and Cosmology, Ministry of Education; Shanghai Key Laboratory for Particle Physics and Cosmology; Institute of Nuclear and Particle Physics, Shanghai 200240, People's Republic of China

^f Also at Key Laboratory of Nuclear Physics and Ion-beam Application (MOE) and Institute of Modern Physics, Fudan University, Shanghai 200443, People's Republic of China

^g Also at State Key Laboratory of Nuclear Physics and Technology, Peking University, Beijing 100871, People's Republic of China

^h Also at School of Physics and Electronics, Hunan University, Changsha 410082, China

ⁱ Also at Guangdong Provincial Key Laboratory of Nuclear Science, Institute of Quantum Matter, South China Normal University, Guangzhou 510006, China

^j Also at MOE Frontiers Science Center for Rare Isotopes, Lanzhou University, Lanzhou 730000, People's Republic of China

^k Also at Lanzhou Center for Theoretical Physics, Key Laboratory of Theoretical Physics of Gansu Province, Key Laboratory of Quantum Theory and Applications of MoE, Gansu Provincial Research Center for Basic Disciplines of Quantum Physics, Lanzhou University, Lanzhou 730000, People's Republic of China

^l Also at Ecole Polytechnique Federale de Lausanne (EPFL), CH-1015 Lausanne, Switzerland

^m Also at Helmholtz Institute Mainz, Staudinger Weg 18, D-55099 Mainz, Germany

ⁿ Also at Hangzhou Institute for Advanced Study, University of Chinese Academy of Sciences, Hangzhou 310024, China

^o Currently at Silesian University in Katowice, Chorzow, 41-500, Poland

^p Also at Applied Nuclear Technology in Geosciences Key Laboratory of Sichuan Province, Chengdu University of Technology, Chengdu 610059, People's Republic of China
